Building Simulation

Seventh International IBPSA Conference
Rio de Janeiro, Brazil
August 13-15, 2001

ON THE NATURAL DISPLACEMENT VENTILATION FLOW THROUGH A FULL SCALE ENCLOSURE, DRIVEN BY A SOURCE OF BUOYANCY AT FLOOR LEVEL

S. A. Howell and I. Potts
University of Newcastle upon Tyne
Newcastle upon Tyne, NE1 7RU, England

ABSTRACT

This paper presents experimental data for the temperature stratification established within a full-scale enclosure, for the natural displacement ventilation flow driven by a source of buoyancy at floor level within the space with air as the working fluid.

A range of predictive techniques is also investigated for the flow, and for each technique a critical comparison with the experimental data is presented.

It is confirmed that the salt-bath modelling technique and related mathematical model of Linden et, al. (1990) is not appropriate for the prediction of this type of ventilation flow in full-scale buildings.

Computational fluid dynamics is a powerful technique that can yield realistic predictions for this type of ventilation flow. Even this approach, however, requires further investigation before it can be used routinely. In particular, this paper illustrates the effect of applying different models of turbulence, and highlights the requirement to employ a complete thermal radiation model when using the CFD technique to predict this class of flow.

INTRODUCTION

Almost half of the total energy consumption in the UK is used in buildings, and this is dominated by electricity use for heating, ventilation, air-conditioning and lighting systems (CIBSE, 1998). Clearly, if more environmentally friendly strategies could by employed for the design of the building services, such as the provision for ventilation by natural means, then this energy consumption, together with the related emissions of carbon dioxide which account for three-quarters of all greenhouse gas emissions, could be significantly reduced.

One of the major barriers to the natural ventilation approach is the lack of a reliable design tool for such flows. Linden and his co-workers (University of California, previously at the University of Cambridge) have developed some simple mathematical models for natural displacement ventilation of an enclosure over the past decade. This work has recently been reviewed (Linden, 1999). The models are validated using the salt-bath technique, which uses salt water to generate density differences and motivate the displacement flow.

This paper reports independent validation work, where a natural displacement ventilation flow, driven by a source of buoyancy at floor level, is established within a full-sized enclosure with air as the working fluid. This is an extension of previously published work (Howell and Potts, 1998), where a smaller scale enclosure was studied. The current investigation is, however, truly representative of the ventilation flows observed in real buildings.

It is found that there are differences between the ventilation flow through the full-scale test room and that predicted by the simple mathematical models for the steady-state case. The causes of the differences are identified and discussed.

Computational fluid dynamics is a powerful predictive technique that can realistically describe natural ventilation flows within buildings. Even this approach, however, requires further investigation to ensure that useful predictions are obtained. A major problem is the validity of the turbulence models that must be employed for ventilation simulations. A wide variety of flow regimes are observed in many buildings, and it is apparent that as yet, no single model of turbulence can accurately describe the range of features generally found in room turbulence. In addition, a simulation should incorporate a model to account for the effects of heat transfer due to thermal radiation.

Numerical predictions of the ventilation flow through the test room have been performed using a CFD computer code, and are compared with the flow through the enclosure. A variety of turbulence models are employed for the computer simulations, together with a model for thermal radiation, and the predictions obtained are compared and discussed.

The experimental results obtained from the test room form a useful set of benchmark data for the validation of CFD codes that are intended to be used for the investigation of buoyancy-driven ventilation flows through full-scale enclosures.

EXPERIMENTAL SETUP

The experimental test-room was representative of a full-sized office space. This was a natural

extension to the previous experimental investigation of Howell and Potts (1998).

The test-room was constructed within a large chamber at the University of Newcastle. The chamber provided two essential features for the experimental work. Firstly, the envelope of the chamber was well sealed, so that any interference due to external wind effects was minimised.

Secondly, the physical dimensions of the chamber were large compared with those of the test-room, so that the walls of the chamber did not affect the ventilation flow through the test-room. Indeed, the height of the chamber was about two and a half times that of the test-room, and there was sufficient room at the end walls of the test-room so that the flow through the openings was unaffected by the presence of the boundaries of the chamber.

The test-room was assembled from standard 2440x1220mm sheet materials attached to an aluminium frame. The frame was constructed from 'Dexion' slotted angle, and sheets of chipboard bolted to the frame form the walls, ceiling and floor of the enclosure. Any gaps at joints between the panels were sealed, so that the test-room was airtight. The internal surfaces of the test-room were painted matt white. The floor of the test-room was raised 100mm above the existing concrete floor of the wind tunnel chamber in order to prevent the thermally massive floor from significantly affecting the airflow within the test-room.

The end walls were manufactured from polycarbonate sheet, so that the inside of the enclosure was visible from outside. It is these walls which incorporated the openings to the enclosure. The size of each opening could be adjusted by sliding a polycarbonate panel to the required position, the panel being secured in place by a channel machined into the structural batten used to keep the polycarbonate sheet rigid.

A 225W plate heater measuring 0.4×0.2m was positioned in the centre of the floor to provide the heat source.

Measurements of air temperature were performed extensively throughout the test-room using twelve Platinum resistance thermometers. One of the thermometers was positioned in the inlet region to record the temperature of the air entering the test-room. The remaining thermometers were mounted on a vertical mast, in order to obtain the instantaneous vertical temperature profile at any particular position. The mast was supported by a frame, which itself was supported by rollers engaged on guide rails, so that it could be accurately traversed along the x-axis of the test-room. The frame was positioned from outside the enclosure by means of a pulley and rope system, and the guide rails had periodic notches machined into the upper edge for accurate and repeatable location of the frame.

Each resistance thermometer formed one leg of a bridge circuit, and had a resistance of 100Ω. The supply voltage to the bridge was maintained at 100mV, so that resistive heating of the element was insignificant.

The imbalance voltage across the bridge provided a measure of the change in resistance of the resistive thermometer element and therefore of temperature. The imbalance voltage was monitored by a programmable amplifier, with a gain of 1000, and was then converted to a digital signal, which was subsequently transferred to a PC for further analysis.

The thermometers were calibrated using a water-bath and a mercury-in-glass thermometer, which was accurate to within 0.1K. Although the platinum temperature-resistance relationship for the thermometer elements was quadratic in nature, for the small changes in temperature which occurred within the test-room, it was acceptable to assume a linear relationship without introducing significant error. Calibration was performed at two temperatures, one at each end of the range of temperatures expected during the experiments. Assuming a linear variation of temperature with resistance, a third temperature in the middle of the expected range was measured. The range of temperatures measured by the thermometers was less than one-tenth of a degree Kelvin.

SIMULATIONS

Computer simulations of the flow through the test-room were performed using the Computational Fluid Dynamics package Fluent, version 5.4. This is an unstructured code, which allows the engineer much more freedom in terms of grid density.

Fluent 5 employs a collocated grid arrangement, together with Rhie-Chow interpolation (Rhie and Chow, 1983) to prevent non-realistic oscillations developing in the pressure field as the simulation proceeds. Pressure-velocity coupling was achieved using the SIMPLEC algorithm (van Doormaal and Raithby, 1984).

The third-order QUICK differencing scheme (Leonard, 1979) was used to evaluate the convection terms for the Navier-Stokes equations, the energy equation and the turbulent transport equation, in order to reduce numerical diffusion which is generally more significant on an unstructured grid. Linear interpolation was used to determine the face pressures required for the source terms in the discretised Navier-Stokes equations.

The effects of turbulence were modelled in this paper using a variety of two-equation turbulence models. Each model is based upon the eddy viscosity concept and requires additional transport equations to be solved for two new flow variables; the turbulence kinetic energy k and the rate of dissipation of turbulence kinetic energy ε. The models of

turbulence investigated were the standard k-ε model (Launder and Spalding, 1974), the k-ε RNG model (Yakhot and Orzsag, 1986), and the realisable k-ε model (Shih et. al., 1995).

Thermal radiation transfer was modelled in this paper using the discrete-ordinates (DO) radiation model (Raithby and Chui, 1990, Chui and Raithby, 1993). This particular model solves the governing radiative transfer equation for a finite number of discrete solid angles, each of which has an associated fixed vector direction. The radiative transfer equation is transformed into a transport equation for radiation intensity in a particular vector direction, which is solved using the same solution method that is used for solving the Navier-Stokes and energy equations. The DO model, however, must solve for as many transport equations as there are directions, so that this model can quickly become computationally intensive. In addition, the radiation intensity in each vector direction must be stored at each iteration, so that memory and storage requirements are significantly increased. For the simulations presented in this paper, the DO model was solved for 32 vector directions.

Pure gases such as nitrogen and oxygen are essentially transparent to thermal radiation. The water vapour in air, however, can absorb and emit radiation, and this should be taken into account when modelling radiation transfer. The absorption coefficient for water vapour in air is taken to be 0.17 (ASHRAE, 1977).

In the previous study (Howell and Potts, 1998) it was established that the k-ε RNG model of turbulence provided the best predictions of temperature stratification for the smaller test-rig. It is also the view of others (Chen, 1995) that this model of turbulence should be employed for the simulation of building ventilation flows. The k-ε RNG model is therefore used for the CFD simulations incorporating the effects of thermal radiation.

The grid used for the simulations, which consisted of approximately 150,000 computational cells, is illustrated in Figure 2. The test-room is modelled as an enclosure within the larger chamber, obviating the need to apply specific boundary conditions in the region of the openings to the room. Only a quarter of the domain was modelled, with planes of symmetry defined along the x- and z-axes of the test-room. In the simulations that employed a turbulence model, the standard wall-function approach (Launder and Spalding, 1974) was used to model the region adjacent to the walls of the test-room and the floor of the chamber. Also, in the simulations including the DO radiation model, the surfaces of the walls of the room were assumed to have an absorption coefficient of 0.85 (ASHRAE, 1977). Constant static-pressure boundary conditions were used to model the remaining boundaries of the grid. A wall boundary condition with a specified constant heat flux was used to model the 225W heat source.

EXPERIMENTAL RESULTS

The experimental results obtained thus far are presented in Figure 3 and Figure 4. The figures show the average difference in temperature between the reference thermometer located in inlet B and each of the thermometers located on the mast for the two halves of the room, either side of the plume, henceforth designated section A and section B (Figure 1). An example of the temperature difference along the entire x-axis of the test-room is given in Figure 5.

It is observed that the flow in the test-room is not precisely symmetrical about the z-axis. This is due to the fact that air entering the room at inlet A is consistently about quarter of a degree cooler than air entering at inlet B, due to the imperfect construction of the surrounding chamber. As a consequence of this, the plume leans slightly towards the B-end of the test-room.

The lack of symmetry can be assessed by comparing the temperature profiles presented in Figure 3 and Figure 4. It is observed that the lack of symmetry manifests itself mainly at the lowest level of the test-room, within 0.3m of the floor, and to a lesser extent at the highest level, within say 0.4m of the ceiling. For the remainder of the space, however, the temperature field is indeed approximately symmetrical.

ANALYSIS OF RESULTS

Despite the lack of symmetry within the test-room, it is observed that the temperature profile along sections A and B exhibit the same features. It is observed that for each combination of opening size, the temperature profile features a steep temperature gradient from floor level up to a height of about 1m. Above this height, the temperature gradient is less steep.

The shape of the temperature profile appears to be independent of the effective area of the openings to the test-room. The effective area does, however, influence the actual values of temperature difference. It is observed that as the effective area is reduced, the values of temperature difference increase. This is to be expected, since if the area of the openings is reduced, the volume flow rate through the test-room will also reduce. From the first law of thermodynamics, therefore, the air temperatures within the test-room must increase.

COMPARISON OF RESULTS WITH PREVIOUS WORK

From a comparison of Figure 3, Figure 4 and Figure 7 it is observed that the nature of the

temperature profile in the full-scale test-room is different to that in the smaller scale test-rig previously studied (Howell and Potts, 1998). It is thought that this difference is due to the non-reflection of thermal radiation in the experiments within the smaller scale test-rig, since all of the walls of the small rig were manufactured from transparent polycarbonate sheet.

COMPARISON OF RESULTS WITH THE MATHEMATICAL MODEL

From a comparison of Figure 3, Figure 4 and Figure 6 it is clear that the mathematical model of Linden et. al. (1990) does not realistically describe the distribution of temperature within the full-scale test-room. Whereas the model predicts a sharp interface between two layers of air of differing temperature, the experimental results show that no such interface occurs.

This difference in temperature profile is due to the mechanisms for the transport of heat present within the test-room. The mathematical model neglects both diffusion of heat and thermal radiation, so that the only remaining mechanism for heat transfer is convection. This is the basis for the assumption that two layers of air of differing temperatures can co-exist in the same confined space without any diffusion over the sharp interface.

Good agreement has been reported between the mathematical model and validation studies using the salt-bath technique (Linden et. al., 1990). This is because the salt-bath technique also neglects the mechanisms of thermal radiation and diffusion.

Whilst the kinematic viscosity of water is only about one-tenth that of air, the diffusivity of salt in water is less than one ten-thousandth that of heat in air (Lane-Serff, 1989). The salt-bath technique is, therefore, only suitable for modelling flows where diffusion of heat is insignificant, since salt diffuses too slowly in water to represent the diffusion of heat in air.

Furthermore, a review of experimental work on differentially heated cavities, it has been reported (Olson et. al., 1990) that significant differences in temperature profile and flow pattern occur, depending upon whether the experimental fluid is water or a gas. It is suggested that the absence of thermal radiation in the water experiments may contribute to the differing results. If this is true, then the absence of thermal radiation with the salt-bath technique will also affect the predictions to some extent.

It is perhaps not surprising, therefore, that the validation studies using the salt-bath technique and the mathematical model are in good agreement.

In the full-scale enclosure, however, diffusion of heat is a significant mechanisms of heat transfer. Molecular diffusion is important, and this is augmented by turbulent diffusion within the space. In addition, the differences in the experimental data for the full-scale test-room and the smaller test-rig suggest that thermal radiation is also a significant mechanism for heat transfer.

The salt-bath technique is, therefore, not appropriate for modelling the ventilation flow through the full-scale test-room, or indeed for ventilation flows in buildings in general, where all three mechanisms of thermal transport coexist.

COMPARISON OF RESULTS WITH CFD SIMULATIONS

The CFD predictions for two example simulations, with effective area of opening $A^* = 0.18m^2$ and $A^* = 0.48m^2$, are presented in Figure 8 and Figure 9 respectively. For each simulation, the effects of thermal radiation have been neglected. Each prediction illustrates the effect of different turbulence models upon the prediction of the temperature stratification within the enclosure.

A comparison of the experimental data (Figure 3 and Figure 4) with the CFD predictions show that the CFD technique is an improvement upon the mathematical model and salt-bath techniques for the prediction of full-scale ventilation flows.

The CFD result for the smaller opening ($A^* = 0.18m^2$) exhibits a steep temperature gradient in the lower portion of the room, with a region where the temperature gradient is less steep above. This is in qualitative agreement with the experimental results. The height at which the temperature gradient change, and the overall change in temperature between floor level and ceiling level is not in agreement with the experimental data.

The CFD result for the larger opening ($A^* = 0.48m^2$) shows a region of constant temperature at low level within the room, with a steep temperature gradient above, and a region where the temperature gradient is less steep at high level. This is not a particularly good agreement with the experimental results. The overall change in temperature between floor level and ceiling level is, however, in reasonable agreement with the experimental data.

From Figure 10 and Figure 11 it is clear that the incorporation of the thermal radiation model can dramatically improve the CFD predictions with respect to the experimental data. In addition, it is apparent that the absorption coefficient of the gas, which effectively depends upon the relative humidity within the space, is crucial to the success of a CFD prediction.

The profile of temperature difference for the smaller opening ($A^* = 0.18$, Figure 10) with the application of the DO-radiation model, and the absorption coefficient of air set to 0.17 is in excellent agreement, both qualitatively and quantitatively, with

the experimental data from the full-scale test-room. The prediction manifests a steep temperature gradient from floor level up to a height of about 1m, and the temperature gradient is less steep above this height. The temperature difference between ceiling level and floor level is predicted to be about two and a quarter degrees Kelvin, which corresponds to the experimental results.

The profile of temperature difference for the larger opening ($A^* = 0.48$, Figure 11) with the DO-radiation model, and the absorption coefficient of air set to 0.17 is also in good agreement with the experimental data. It shows a steep temperature gradient in the lower region of the room, with a less steep temperature gradient in the higher region. The temperature difference between ceiling and floor levels is predicted to be about two degrees Kelvin, which again corresponds to the experimental results.

CONCLUSIONS

In this paper extensive measurements providing information regarding temperature profile within a full-scale test-room are presented for the case of a natural displacement ventilation flow driven by a source of buoyancy at floor level within the room. The nature of the temperature stratification within the full-scale room differs from that measured in a smaller-scale test-rig. The cause of the difference is thought to be the non-reflection of thermal radiation at the wall boundaries in the small-scale experiment.

The experimental data presented has been used to assess a range of alternative prediction techniques for this type of flow. It is apparent that the salt-bath technique and the associated mathematical model of Linden et. al. (1990) are not appropriate for the prediction of this class of flow. The predictions obtained from these techniques do not realistically describe the distribution of temperature within the full-scale test-room. This is because both predictive techniques neglect thermal radiation and diffusion as mechanisms for thermal transport. For the flow through the test-room, however, thermal radiation and diffusion are thought to significantly affect the temperature stratification within the space.

Computational fluid dynamics remains as a powerful technique for the prediction of the class of flow considered in this paper - natural displacement ventilation flows through enclosures. The CFD predictions must be performed, however, with the application of suitable models for both turbulence and thermal radiation effects. In addition, the absorption characteristics of air, due to concentration of water vapour in the atmosphere, must be properly assessed and included as part of the simulation if a realistic prediction is to be generated.

ACKNOWLEDGEMENTS

This work was sponsored by consulting engineers Cundall Johnston and Partners, Regent Centre, Gosforth, Newcastle upon Tyne, NE3 3LU, England.

REFERENCES

ASHRAE, 1977, "Fundamentals ASHRAE Handbook", (Atlanta, GA: American Society of Heating, Refrigeration and Air Conditioning Engineers)

Chen, Q., 1995, "Comparison of different k-ε models for indoor air flow computations", *Numer. Heat Transfer*, B28:353-369

Chui, E. H., and Raithby, G. D., 1993, "Computation of radiant heat transfer on a non-orthogonal mesh using the finite-volume method", *Numer. Heat Transfer*, B23:269-288

CIBSE, 1998, "Energy efficiency in buildings CIBSE Guide", (London: Chartered Institution of Building Services Engineers)

Howell, S. A., and Potts, I., 1998, "A comparison of predictive techniques for natural displacement ventilation of buildings", *Proc. CIBSE Nat. Conf.*:156-164

Lane Serff, G. F., 1989, "Heat flow and air movement in buildings", Ph.D. thesis, Cambridge Univ., UK

Launder, B. E., and Spalding, D. B., 1974, "The numerical computation of turbulent flows", *Comput. Methods Appl. Mech. Eng.* 3:269-289

Leonard, B. P., 1979, "A stable and accurate convective modelling procedure based on quadratic upstream interpolation", *Comput. Methods Appl. Mech. Eng.* 19:59-98

Linden, P. F., 1999, "The fluid mechanics of natural ventilation", *Annu. Rev. Fluid Mech.* 31:201-238

Linden, P. F., Lane Serff, G. F., and Smeed, D. A., 1990, "Emptying filling boxes: the fluid mechanics of natural ventilation", *J. Fluid Mech.* 212:309-335

Olson, D.A., Glicksman, L. R., and Ferm, H. M., 1990, "Steady-state natural convection in empty and partitioned enclosures at high Rayleigh numbers", *ASME J. Heat Transfer* 112:640-647

Raithby, G. D., and Chui, E. H., 1990, " A finite-volume method for predicting a radiant heat transfer in enclosures with participating media", *ASME J. Heat Transfer* 112:415-423

Rhie, C. M., and Chow, W. L., 1983, "Numerical study of the turbulent flow past an airfoil with trailing edge separation", *AIAA Journal* 21(11):1525-1532

Shih, T. H., Liou, W. W., Shabbir, A., and Zhu, J., 1995, "A new k-ε eddy-viscosity model for high Reynolds number turbulent flows - model

development and validation", *Comput. Fluids* 24(3):227-238

Van Doormaal, J. P., and Raithby, G. D., 1984 "Enhancements of the SIMPLE method for predicting incompressible fluid flows", *Numer. Heat Transfer*, 7:147-163

Yakhot, V., and Orzsag, S. A., 1986, " Renormalization group analysis of turbulence: I. basic theory", *J. Sci. Comp.* 1:1-51

NOMENCLATURE

A^* = effective area of the openings to the enclosure. From Linden et. al. (1990)

$$A^* = \left(\frac{A_i A_o}{\sqrt{A_i^2 + A_o^2}} \right) \sqrt{2} ,$$

where A_i and A_o are the areas of the low-level opening and high-level opening respectively.

FIGURES

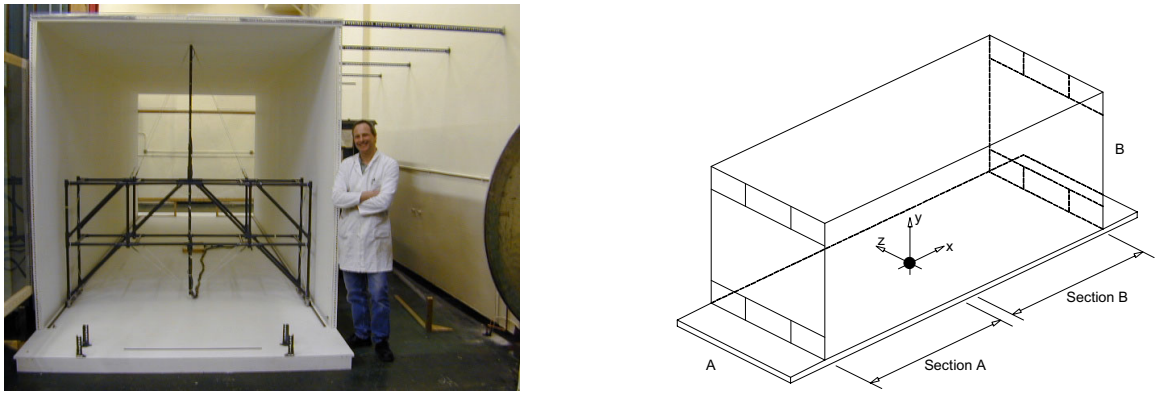

Figure 1 - Experimental test-room and associated co-ordinate system

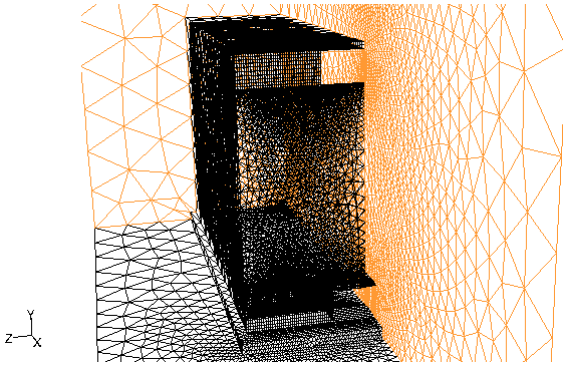

Figure 2 - Computational grid used for CFD simulations

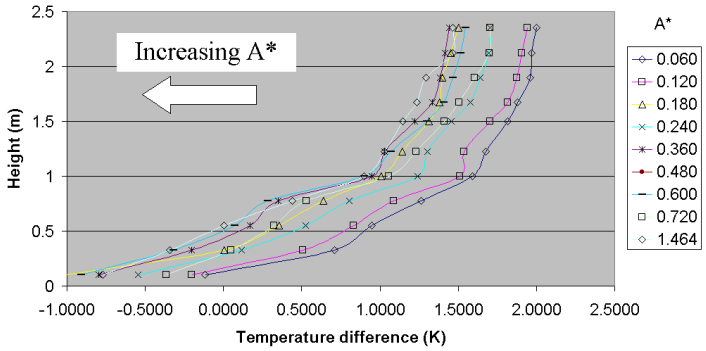

Figure 3 - Temperature profiles within the test-room for section A

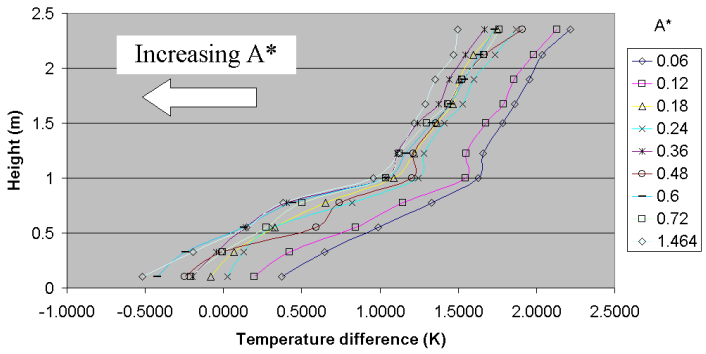

Figure 4 - Temperature profiles within the test-room for section B

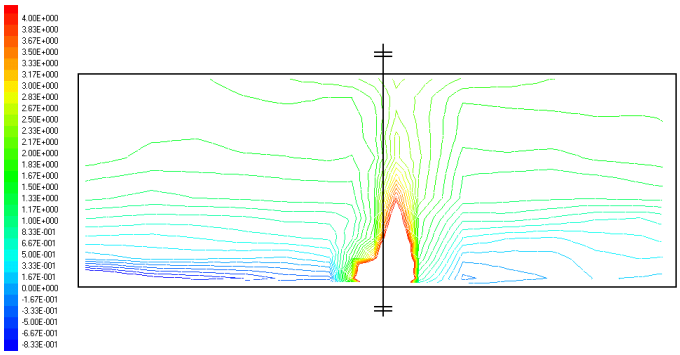

Figure 5 - Plot of temperature difference along the x-axis of the test-room for an effective area A* = 0.18

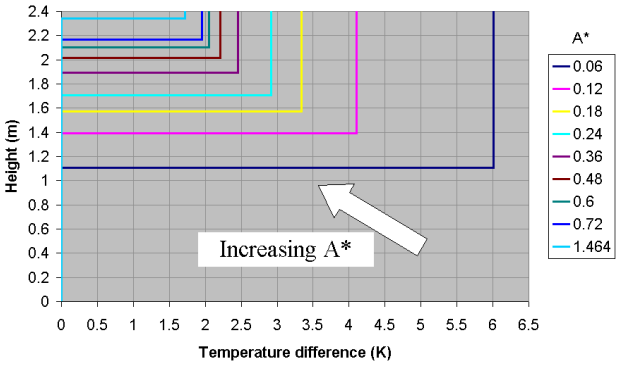

Figure 6 - Temperature profiles predicted by the mathematical model of Linden et. al. (1990)

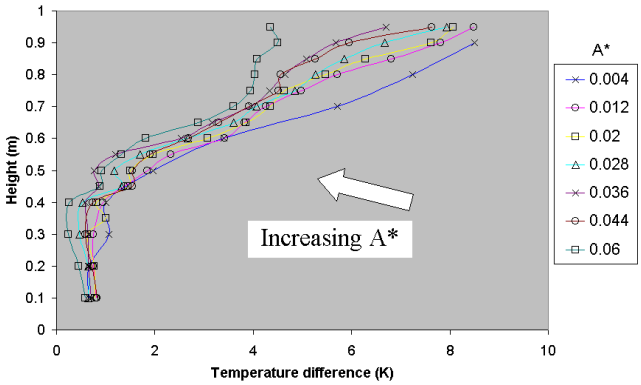

Figure 7 - Temperature profiles within the small scale test-rig (Howell and Potts, 1998)

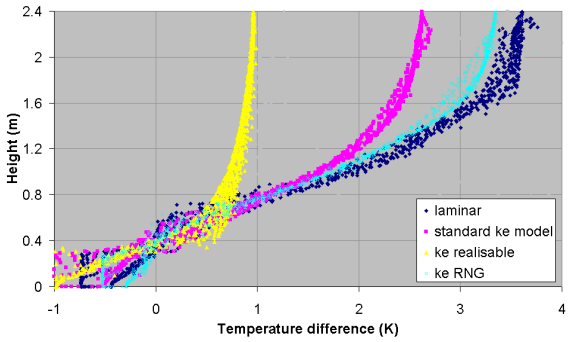

Figure 8 - Temperature profiles predicted by CFD simulation, using a variety of turbulence models, for an effective area of opening A* = 0.18

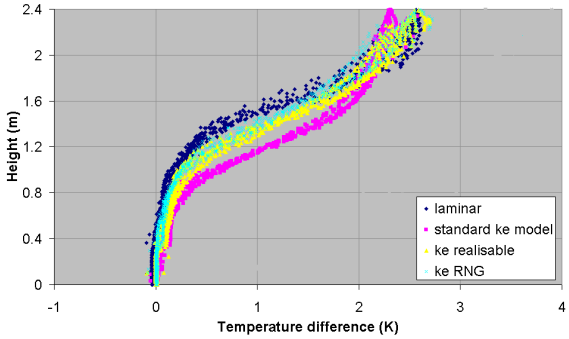

Figure 9 - Temperature profiles predicted by CFD simulation, using a variety of turbulence models, for an effective area of opening A* = 0.48

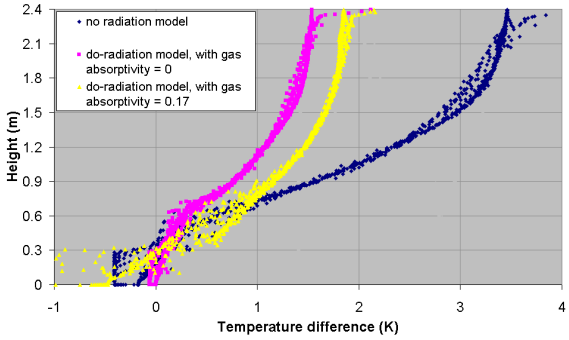

Figure 10 - Temperature profiles predicted by CFD simulation, using the k-e RNG turbulence model together with the discrete-ordinates radiation model, for an effective area of opening A* = 0.18

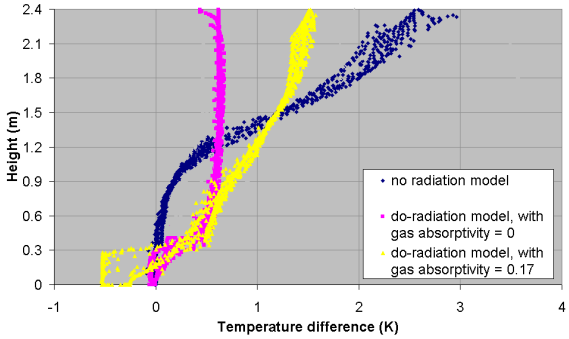

Figure 11 - Temperature profiles predicted by CFD simulation, using the k-e RNG turbulence model together with the discrete-ordinates radiation model, for an effective area of opening A* = 0.48